



HARMONIZED APPROACH TO STRESS TESTS FOR CRITICAL INFRASTRUCTURES AGAINST NATURAL HAZARDS (STREST)

A. Mignan⁽¹⁾, D. Giardini⁽²⁾, F. Cotton⁽³⁾, I. Iervolino⁽⁴⁾, B. Stojadinovic⁽⁵⁾, K. Pitilakis⁽⁶⁾

⁽¹⁾ Senior Researcher, Institute of Geophysics, Swiss Federal Institute of Technology (ETH) Zurich, arnaud.mignan@sed.ethz.ch

⁽²⁾ Professor, Institute of Geophysics, Swiss Federal Institute of Technology (ETH) Zurich, domenico.giardini@erdw.ethz.ch

⁽³⁾ Professor, GFZ German Research Center for Geosciences and Potsdam University, fabrice.cotton@gfz-potsdam.de

⁽⁴⁾ Professor, Dip. di Strutture per l'Ingegneria e l'Architettura, Università degli Studi di Napoli Federico II, iunio.iervolino@unina.it

⁽⁵⁾ Professor, Institute of Structural Engineering, Swiss Federal Institute of Technology (ETH) Zurich, stojadinovic@ibk.baug.ethz.ch

⁽⁶⁾ Professor, Aristotle University, Thessaloniki, kpitilak@civil.auth.gr

Abstract

Critical Infrastructures (CIs) provide essential goods and services for modern society; they are highly integrated and have growing mutual dependencies. Recent natural events have shown that cascading failures of CIs have the potential for multi-infrastructure collapse and widespread societal and economic consequences. Moving toward a safer and more resilient society requires improved and standardized tools for hazard and risk assessment of extreme events, and their systematic application to whole classes of CIs. Among the most important assessment tools are the stress tests, designed to test the vulnerability and resilience of individual CIs and infrastructure systems in natural disasters. We present the main results of the STREST project regarding extreme event quantification with focus on extreme earthquakes and extreme earthquake consequences. We show that extremes result from the combination of stochastic, site-specific and/or explicit physical processes. The stochasticity of earthquake risk is represented by random phenomena (e.g., random earthquake clusters, spectral acceleration sigma) and model uncertainties. Site-specific aspects include geotechnical properties, near-source effects and ground shaking spatial correlations, which can locally increase the seismic risk. Finally, physical processes include maximum fault rupture propagation, earthquake interactions (i.e., aftershocks) and associated vulnerability changes, inter-hazard interactions (e.g., tsunamis, landslides), natech interactions (i.e., domino effects within the CI system following an earthquake), and additional CI interactions. Combination of all these processes tends to yield more extremes (fattening the risk curve) based upon which the CI stress test is made. The different steps of the STREST stress test method are presented in a companion paper.

Keywords: Extreme; critical infrastructure; stress test; uncertainty; multi-risk.

1. Introduction

The “Harmonized approach to stress tests for critical infrastructures against natural hazards” (STREST) project (2013-2016, www.strest-eu.org) aimed at investigating the main processes that could exacerbate earthquake hazard and risk (i.e. extremes or tail events) and which should therefore be considered in the stress tests of critical infrastructures (CIs). Taking as example the 2011 Fukushima disaster, some of the main issues leading to this catastrophe were the incorrect evaluation of the earthquake maximum magnitude and of the domino effects across the different elements of the nuclear power plant (NPP) extended system [1]. The need for “a targeted reassessment of the safety margins” of CIs has since then become very clear [2]. This targeted reassessment does not only apply to NPPs but to other types of CIs. The CIs considered in the STREST project are reported in Table 1 and pictured in Fig. 1. The CIs are categorized into three classes: (A) individual, single-site infrastructures with high risk and potential for high local impact and regional or global consequences; (B) distributed and/or geographically-extended infrastructures with potentially high economic and environmental impact; and (C) distributed, multiple-site infrastructures with low individual impact but large collective impact or dependencies. In the present paper, we show that extremes result from the combination of stochastic, site-specific and/or explicit physical processes. These processes are listed in Table 1 and described individually in the following sections.



Fig. 1 – The six critical infrastructures (CIs) considered in the STREST project.

2. Extremes emerging at the natural hazard level

2.1 Model uncertainties (stochastic process)

The most popular framework to account for model uncertainties is the logic tree [3; 4]. Fig. 2 shows an example of logic tree that describes different Peak Ground Velocity (PGV) ground motion models calibrated to induced seismicity (our CI-B2 Groningen gas network case). This simple example shows that PGV varies within two orders of magnitude when considering the full range of the logic tree (grey curves) for a 3 km deep induced earthquake of magnitude 4. It means that this event is from barely perceptible to strongly perceptible by the local population [5]. These uncertainties can however be reduced by taking into account regional geotechnical properties (see section 2.4; black curves in Fig. 2). Model uncertainty (at both hazard and risk levels) is a well-known issue, therefore not discussed in more detail here. Let us just note that adding more knowledge may lead to uncertainty increase (i.e. model diversification) or reduction (i.e. model convergence, site-specific data). However, in both cases, there is no *a priori* trend in the overall hazard evolution. Model uncertainty is therefore not an exacerbating process that would systematically generate more extreme events, in contrast with some other processes described below. As shown in the STREST companion paper, the evaluation of model uncertainty is required at most levels of the CI stress test framework.

Table 1 – Potentially exacerbating hazard and risk processes considered at different non-nuclear CIs

CI class	A		B			C
CI type	1. Petrochemical plant	2. Hydropower dam	1. Oil pipeline	2. Gas distribution network	3. Port infrastructure	1. Industrial district
Location	Milazzo, IT	Valais, CH	Turkey	Groningen, NL	Thessaloniki, GR	Tuscany, IT
Processes common to hazard & risk						
Model uncertainties	✓	✓	✓	✓	✓	✓
Natural hazard processes						
Ground motion sigma					✓	
Coinciding events		✓				✓
Geotechnical properties				✓	✓	
Near-source effects	✓		✓			
Spatial correlations			✓	✓	✓	✓
Rupture propagation			✓		✓	
Hazard interactions	✓	✓				✓
Industrial hazard & risk processes						
Damage-dependent vulnerability	✓	✓				✓
Natech & CI element interactions	✓	✓			✓	

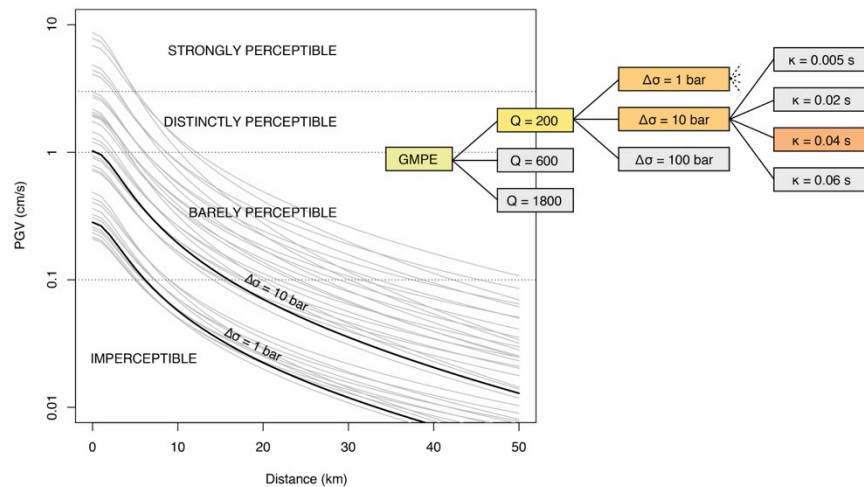


Fig. 2 – Logic tree with the attenuation functions proposed by [6] for induced seismicity. Considering a stress drop $\Delta\sigma = 3-17$ bars and the attenuation factors $Q = 20$ and $\kappa = 0.04$ s [7] for the Groningen gas field (CI-B2), both uncertainties and absolute PGV values are reduced (black curves) (for fragility functions of pipelines on the Groningen gas network, see [8]).

2.2 Ground motion sigma (stochastic process)

Probabilistic hazard assessments methods all depend, directly or indirectly, on the probability distributions of input parameters. For example, ground-motion models describe the distribution of ground motion in terms of a median and a logarithmic standard deviation. This standard deviation generally referred to as sigma (σ) exerts a strong influence on the results of probabilistic seismic-hazard analysis (PSHA) for low probabilities of exceedence; because ground-motion parameters are generally log-normally distributed, the value of the predicted ground motion will vary as an exponential function of any positive or negative increment in the value of sigma. Sigma has become a topic of particular importance in the evaluation of ground motions used for the design of CIs. The availability of well-recorded ground motions at single sites from multiple earthquakes in the same regions has allowed refining this ground-motion variability used for simulations [9] or site-specific analyses [10]. These new databases also give the opportunity to better evaluate the correlation of ground motion across spectral periods [11]. Site-specific correlation models, taking into account magnitude and region dependencies, have been developed for Europe. These correlation models have also been used to derive site-specific conditional site spectra. While the expected loss (if additive) remains unchanged, the variance is underestimated if the correlations discussed above are neglected.

2.3 Coinciding events (stochastic process)

Coinciding events can be defined as the random occurrence of more than one event within a relatively small spatiotemporal window. The probability of a cluster composed of X events is the product of the individual probabilities of occurrence. While random clusters are rare by their nature, they concentrate hazard in space and time and participate to an increase in scenario complexity with $(n+X-1)!/(X!(n-1)!)$ possible combinations (with possible event repeats) in a pool of n possible events. Due to the hazard concentration, risk effects are non-linear with the losses due to the cluster expected loss not necessarily the sum of the individual event expected losses (see section 3.1). Coinciding events are likely to exacerbate the risk but are rarer than correlated events (for a fixed set of events). Both are investigated in parallel in section 2.8. It should be noted that standard seismic hazard and risk analyses do not consider the case of random combinations of earthquakes due to the rarity of such clusters [12]. These “perfect storm” events can however become relevant in stress tests. They are easy to assess at the hazard level since they follow a basic Poisson process (a Monte Carlo approach becomes useful with increasing n).

2.4 Geotechnical properties (site-specific process)

Site-specific response analyses can be performed to reduce uncertainties in PSHA. An example is shown here for the Thessaloniki Port infrastructures (CI-B3). An extreme earthquake rupture scenario breaking along the whole Anthemountas fault zone with a characteristic magnitude M_w of 7.0 is considered (4975-year return period), including the potential of liquefaction (see also [8]). The median plus one standard deviation spectrum provided by [13] was selected as the target spectrum. Ten synthetic accelerograms were computed to fit the target spectrum, and broadband ground motions were generated to be used as input for non-linear site response analyses using 3D physics-based “source-to-site” numerical simulations. Three representative soil profiles were considered for the site response analysis [14], including in situ geophysical and laboratory tests as well as new array measurements of microtremors. Time-domain 1D equivalent-linear and nonlinear site response analyses including were carried out using the STRATA [15] and Cyclic1D [16] codes. In the latter, the liquefaction model is based on multi-yield-surface plasticity. The uncertainty in the V_s profiles represented by the scatter of the field measurements was evaluated in the simulations, considering a standard deviation of the natural logarithm of the V_s equal to 0.2 in the base-case geotechnical models. Figure 3 presents the derived median and median \pm standard deviation elastic 5% response spectra at the ground surface for one of the selected soil profiles while Figure 4 shows indicative results of the nonlinear site response analysis for the selected input motions for the same soil profile (median V_s profile). From such analysis, we can conclude that the EQL approach predicts significantly larger spectral values (with flatter spectral shapes) compared to the NL spectral shapes, which is due to the fact that the liquefaction model of Cyclic1D can accommodate yielding and permanent ground deformations due to lateral spreading at high strain levels, which may attenuate high-

frequency surface motions. This indicates the complexity of the process, on one side a decrease of ground shaking and on the other side an increase of permanent ground deformation due to liquefaction.

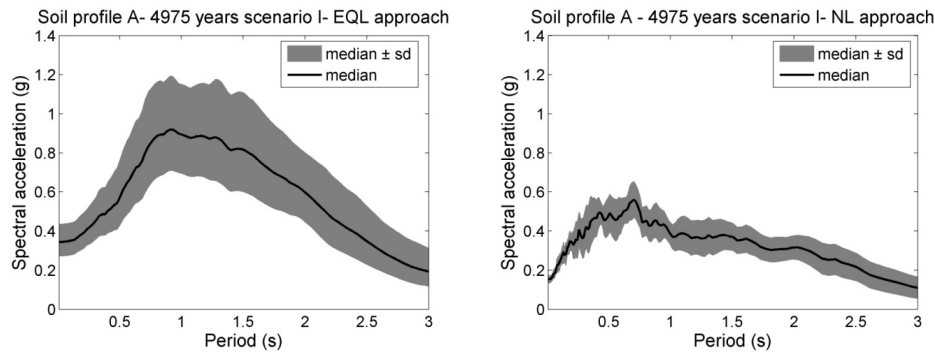


Fig. 3 – Median \pm standard deviation elastic 5% response spectra at the ground surface for one soil profile when using the equivalent linear (EQL) and nonlinear (NL) approaches.

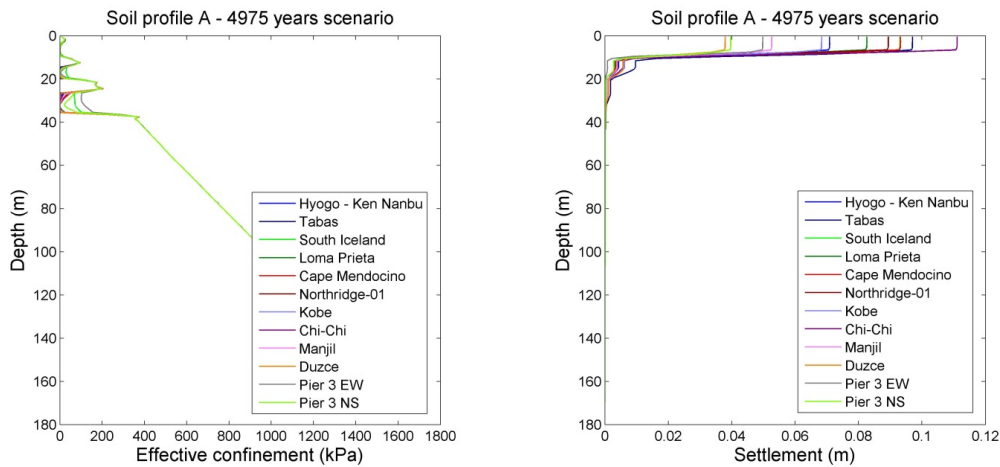


Fig. 4 – Variation of effective confinement (left) and settlement with depth for soil profile (right).

2.5 Near-source effects (site-specific process)

Sites located in proximity to seismic faults are prone to near-source effects related to the geometry of rupture propagation. From a structural engineering point of view, the most important among these phenomena is forward directivity. During fault rupture, shear dislocation can propagate at a speed near shear wave velocity. This can result in wave fronts, generated at different points along the fault, arriving at sites aligned with the direction of rupture propagation (e.g, Fig. 5a) at the same time, delivering most of the seismic energy in a single double-sided pulse registered early in the velocity record (Fig. 5b). Such pulse-like ground motions result in an increase of the amplitudes of elastic and inelastic structural response, for structures within a certain range of periods of natural vibration, which depends on the period of the velocity pulse. In STREST, near-source probabilistic seismic hazard analysis (NS-PSHA) was employed [17] to account for the effect of impulsive motions on seismic actions for structural design. These hazard calculations involved the probabilistic consideration of finite fault rupture scenarios coupled with empirical relations for the probability of pulse occurrence and the resulting amplification of spectral ordinates. Furthermore, a procedure for incorporating this effect into inelastic structural response (and consequently into the design of structures at near-source sites) was proposed [18]. This procedure employs the results of NS-PSHA disaggregation, which provides the conditional probability density of pulse period (Fig. 5c) and the conditional probability of pulse occurrence, given a design scenario. This information is used to calculate the mean value of inelastic demand, according to a semi-empirical equation for pulse-period-dependent inelastic spectra (Fig. 5d). This average inelastic spectral amplification can, in turn, be incorporated

into a static non-linear analysis, providing structural demand for the design scenario. It was shown that at near-source sites, directivity effects could be very influential with respect to structural performance objectives.

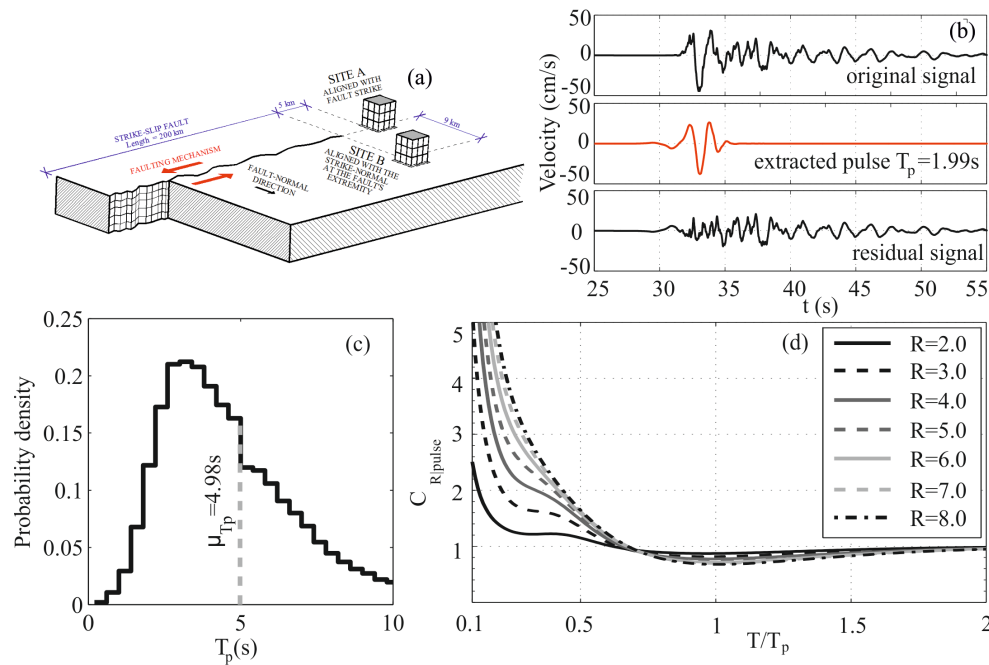


Fig. 5 – Near-source sites with alignment prone to directivity effects (a), velocity time-history of a pulse-like ground motion recorded at AQK station, L’Aquila, Italy, 2009 earthquake (b), probability density of pulse period conditional on a design scenario (c), predictive equation for mean inelastic displacement ratio of pulse-like ground motions (d) adapted from [17,18].

2.6 Spatial correlations (site-specific process)

Monte-Carlo simulations using multi-scale random fields have been developed to incorporate spatial correlations, near-fault directivity effects (section 2.5) and fault permanent displacements. These factors, not taken into account within classical PSHA, are of primary importance for the risk assessment of geographically distributed and extended structures (e.g. pipelines at CI-B1). Annual exceedance rates of dynamic ground-motion intensity measures (GMIMs) (e.g., peak ground acceleration-PGA, peak ground velocity-PGV and spectral acceleration-Sa) as well as permanent fault displacement have been computed taking into account these spacial correlations and directivity effects [19].

2.7 Rupture propagation (physical process)

While earthquake ruptures are known to potentially propagate over several segments (by jumping, bending or branching), fault segments are still modelled as individual faults in standard PSHA models. Only in the most recent version of the Uniform California Earthquake Rupture Forecast (UCERF3) is a process of rupture propagation considered [20]. In STREST, we developed an algorithm to generate sets of cascade ruptures by combining fault segments defined from PSHA models following criteria based on dynamic stress considerations [21] (Fig. 6). These criteria, defined from empirical observations and published dynamic stress simulations, are mainly: (i) a maximum jump distance Δ allowed between segments and (ii) a maximum strike difference δ allowed between two segments. The algorithm outputs cascade ruptures of length L_{max} . The maximum magnitude M_{max} is then estimated using different magnitude-length relationships. Fig. 6 compares the 2013 European Seismic Hazard Model (ESHM13) M_{max} map [22] with the new one of [21] in the case of the Anatolian Peninsula, Turkey (CI-B1; with $\Delta = 10$ km and $\delta = 30^\circ$). The new map indicates an increase of M_{max} from about 0.5 to 1.5. This process yields more extremes by shifting the magnitude upper bound to higher values. While

such events do not control the overall hazard due to low probabilities of occurrence, they must be considered in stress-test what-if scenarios (e.g., in seismic response analysis of buried pipelines at fault crossings [23]).

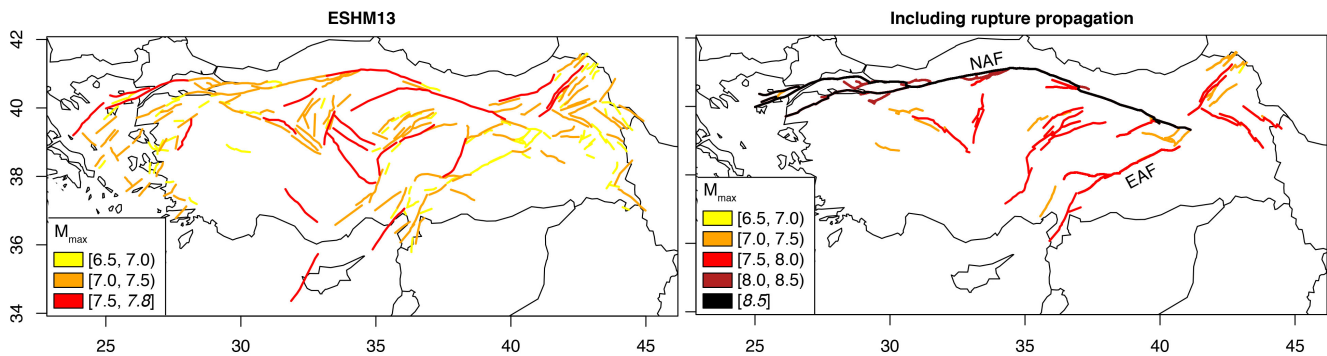


Fig. 6 – M_{max} maps of the Anatolian Peninsula, Turkey (CI-B1); adapted from [21].

2.8 Hazard interactions (physical process)

Hazard interactions can nowadays be systematically included in multi-hazard and multi-risk assessment thanks to Markov Chain Monte Carlo methods [24-26]. Earthquakes can trigger other earthquakes (aftershocks), landslides, tsunamis and various kinds of industrial accidents (see section 3.2). We considered in STREST several cases of hazard interactions, including: (i) earthquake clustering in northern Italy (CI-C1) [25] and (ii) multiple hazard interactions at a Swiss dam (CI-A2) [26]. Fig. 7a shows a simplified ESHM13 fault map of northern Italy and an example of Coulomb stress transfer $\Delta\sigma$ calculation. All $\Delta\sigma$ estimates for trigger/target segment couples were defined in a hazard correlation matrix and the clock changes described by a non-stationary Poisson process [25]. Millions of annual time series were generated for different hypotheses. Results are compared in terms of aggregated damage in Fig. 7b with N_{DS4+} the number of buildings in damage state 4 or 5 (heavy to extreme damage). Here generic building capacity curves were used but precast fragility curves were also developed for STREST (CI-C1) [27-28]. Fig. 7b shows that considering earthquake clustering yields a fattening of the risk curve. This phenomenon becomes important at low probabilities, indicating that standard PSHA may not require such approach. Stress tests should however consider earthquake clustering (both random, section 2.3, and triggered) since it systematically exacerbates the risk compared to the view of considering only individual events [12]. The damage-dependent vulnerability hypothesis is discussed in section 3.1. Hazard interactions at the dam interface are discussed in section 3.2.

3. Extremes emerging at the industrial hazard and risk levels

3.1 Damage-dependent vulnerability (physical process)

Risk assessment of structures subjected to multiple seismic events, for example at the time-scale of weeks/months around a major event, is gathering increasing research attention due to the compelling need for decision makers to have quantitative tools available that enable the management of such a risk. This is because major earthquakes (i.e., mainshocks) typically trigger a sequence of lower-magnitude events clustered in both time and space, which may be damaging for exposed assets. Therefore, risk management for structures in the post-event emergency phase has to deal with this short-term seismicity. Indeed, because the structural systems of interest might have suffered some damage during the mainshock, possibly worsened by damaging aftershocks, the failure risk may be large (e.g., unacceptable) until the intensity of the sequence reduces or the structure is repaired. Fig. 8 sketches out the problem at hand, that is, during an aftershock sequence there may occur threatening events that could further damage an already affected structure, eventually leading to collapse (see also Fig. 7b). This issue may be addressed by modeling the combination of the stochastic processes of damage progression and aftershock occurrence. Recent advancements in PSHA allow assessing hazard of aftershocks following a major event, so-called aftershock probabilistic seismic hazard analysis (APSHA). It was shown that, if a probabilistic model for the vulnerability of structures accumulating seismic damage is available, its combination with APSHA provides a time-variant seismic risk for the structure during the sequence [29]. It is to

note that damage accumulation makes common fragility curves inadequate to tackle this problem. In fact, fragility curves, suitably adapted for this context (e.g., state-dependent fragilities) may be employed in those cases when the damage accumulation is purely state-dependent; e.g., a Markovian process; see [30].

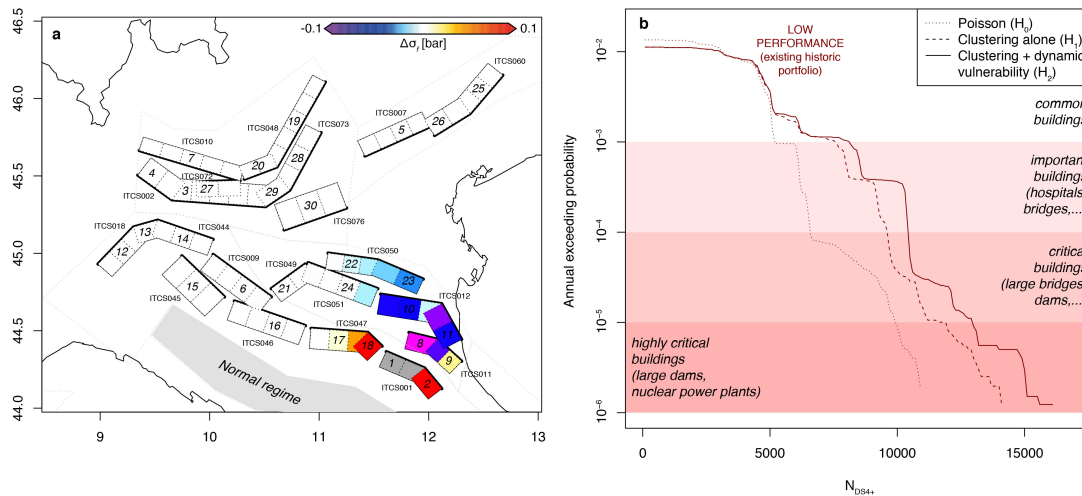


Fig. 7 – a. Fault segments in northern Italy with example of $\Delta\sigma$ field (CI-C1); b. Risk curve showing a tail fattening; adapted from [25].

3.2 Natech and CI element interactions (physical process)

In a complex system, elements are interconnected and their relationship is multifaceted following a specific hierarchy; inter- and intra-dependencies among components and networks are highly affecting the performance of CIs. In general, interactions can be classified as direct, e.g. physical or functional dependencies and indirect, which include cyber, collocation, restoration, substitute, sequential, logical, general and societal dependencies. Their significance is also variable, depending on the type of CI and the functions of interacting components. Assessing the interdependencies in the STREST case studies, it has emerged that physical and geographic dependencies are the most common ones in all the CIs, while direct dependencies are in most cases classified at least as of high significance. The performance of each CI is addressed using appropriate methods and evaluation measures, based on integrated models of critical infrastructure systems [31]. In such models, the dependencies between components and/or systems are accounted for and the systemic performance of the infrastructures (systems or system of systems) is evaluated. As a first example, reference is made to the methods and tools developed for the probabilistic assessment of the systemic performance and loss of harbours exposed to earthquakes (our CI-B3 case), simulating port operations and considering also the interactions among port elements [32]. The analysis is based on an object-oriented paradigm where systems are described through a set of classes, characterized in terms of attributes and methods, interacting with each other [33]. The final goal is to assess the exceedance probability of different levels of performance loss for each system under the effect of any possible seismic input calculated based on the estimated damages and functionality losses of the different components. This output, represents the performance curve (Fig. 9), where the port activity is defined as the total number of containers handled (loaded and unloaded) per day, in Twenty-foot Equivalent Units (TEU). Disaggregation and correlation procedures are also used at a probability level (e.g. design scenario) and loss level (e.g. unacceptable loss, as defined by stakeholders) in order to define the most critical elements for the functionality of the port system. As a second example, the interactions at the dam interface (CI-A2) and impact on outflow and element integrity are given in Fig. 10 [26]. In this case, the Generic Multi-Risk (GenMR) framework was used [24] with interactions between natural events (earthquakes, floods, landslides) and dam element failures (bottom outlet, spillway, hydropower) described in a hazard correlation matrix (see also [34]). Overall we observed that considering interactions led to higher probabilities of dam failure (for a conceptual embankment dam). Yet, those remained far beyond existing safety margins (in Switzerland, CI-A2). For another case of Natech interaction at the STREST CI-A1 site, see [35].

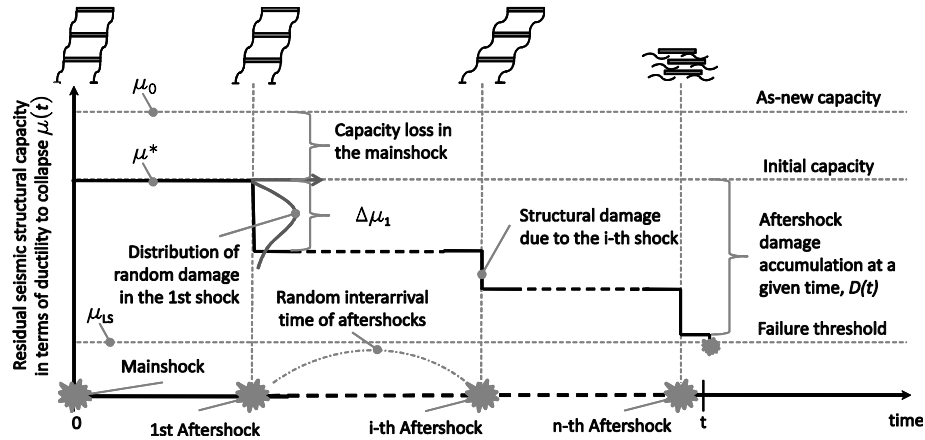


Fig. 8 – Degradation process for a mainshock-damaged structure exposed to aftershocks, adapted from [29].

4. Conclusions

Uncertainties related to the prediction of extreme events are large. We developed methods in STREST to capture those uncertainties but also reduce them – where possible – by a better understanding of underlying stochastic, site-specific and other physical processes. Their combined effects are non-trivial and require full modelling to estimate the overall risk increase (or decrease). These different models may not apply to all types of CIs. A stress test workflow that implements these models is described in the STREST companion paper [36]. The ST@STREST workflow (Fig. 11), comprises four phases: 1) Pre-Assessment phase; 2) Assessment phase; 3) Decision phase; and 4) Report phase. Each phase is subdivided into a number of specific steps, with a total of 9 steps. Three conceptual frameworks, which are termed Stress Test Levels (ST-Ls), have been structured in ST@STREST: ST-L1 based on single-hazard component check, ST-L2 based on single-hazard system-wide Probabilistic Risk Assessment, and ST-L3 based on multi-hazard system-wide Probabilistic Risk Assessment.

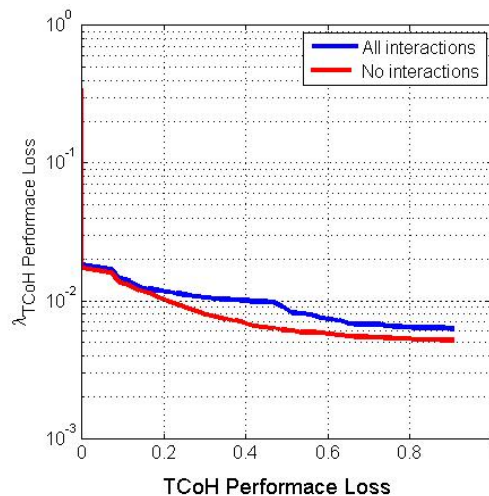


Fig. 9 – Mean annual frequency curves for performance loss of the container terminal at Thessaloniki's port, with and without interaction with electric power network and building collapses [32].

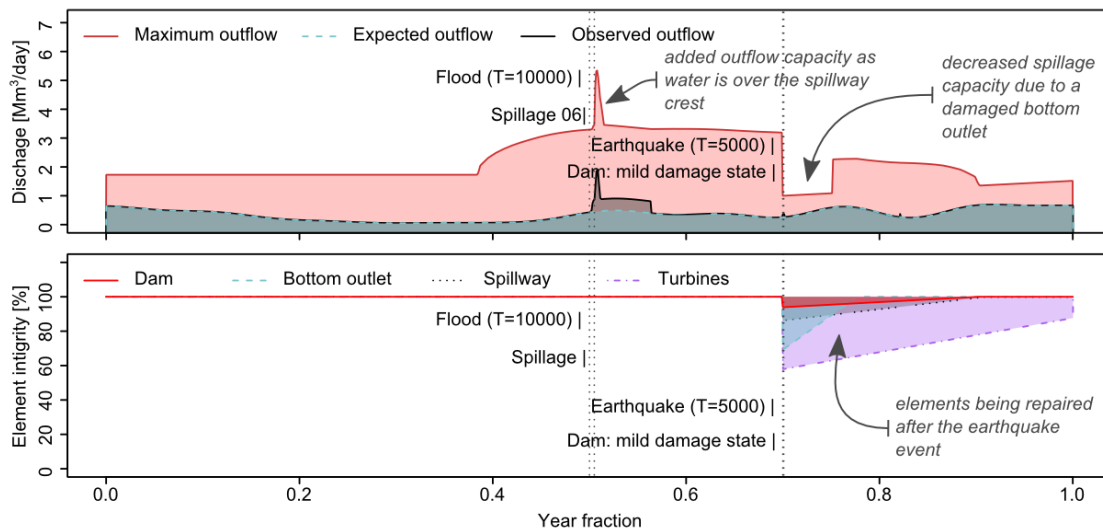


Fig. 10 – Example of dam system response (CI-A2) to extreme flood and earthquake events in the course of one year (outflows on top, element integrities below). Adapted from [26].

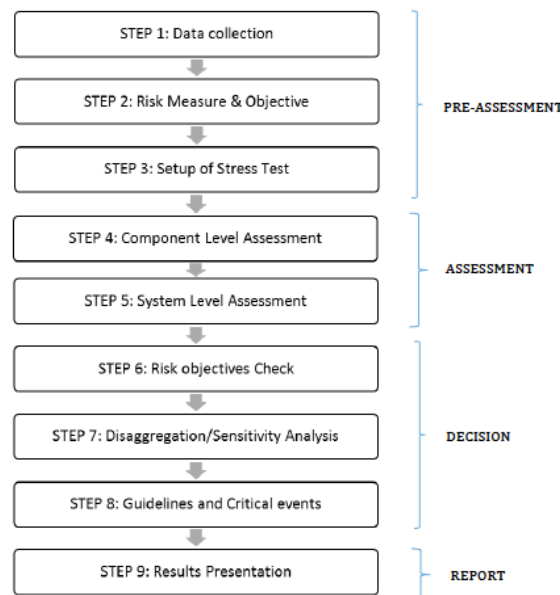


Fig. 11 – Workflow of ST@STREST methodology [36].

5. Acknowledgements

We wish to thank all the members of the STREST consortium for their contributions, and in particular: Stavroula Fotopoulou, Sotiris Argyroudis, Laurentiu Danciu and Ernesto Salzano for their comments on this manuscript. The STREST project was funded by the European Community's Seventh Framework Programme (FP7/2007-2013) under grant agreement no. 603389.

6. References

- [1] Norio O, Ye T, Kajitani Y, Shi P, Tatano H (2011): The 2011 Eastern Japan Great Earthquake Disaster: Overview and Comments. *Int. J. Disaster Risk Sci.*, 2 (1), 34-42.
- [2] European Nuclear Safety Regulators Group (ENSREG) (2011): Declaration of ENSREG. *EU "Stress test" specifications, Annex I, 2011/05/31*, European Nuclear Safety Regulators Group, Brussels, Belgium.

- [3] Marzocchi W, Taroni M, Selva J (2015): Accounting for Epistemic Uncertainty in PSHA: Logic Tree and Ensemble Modeling. *Bull. Seismol. Soc. Am.*, **105** (4), doi: 10.1785/0120140131.
- [4] Mignan A, Landtwing D, Kastli P, Mena B, Wiemer S (2015): Induced seismicity risk analysis of the 2006 Basel, Switzerland, Enhanced Geothermal System project: Influence of uncertainties on risk mitigation. *Geothermics*, **53**, 133-146, doi: 10.1016/j.geothermics.2014.05.007.
- [5] Bommer JJ, Oaets S, Cepeda JM, Lindholm C, Bird J, Torres R, Marroquin G, Rivas J (2006): Control of hazard due to seismicity induced by a hot fractured rock geothermal project. *Engineering Geology*, **83**, 287-306, doi: 10.1016/j.enggeo.2005.11.002.
- [6] Douglas J, Edwards B, Convertito V, Sharma N, Tramelli A, Kraaijpoel D, Mena Cabrera B, Maercklin N, Troise C (2013): Predicting Ground Motion from Induced Earthquakes in Geothermal Areas. *Bull. Seismol. Soc. Am.*, **103** (3), 1875-1897, doi: 10.1785/01201201197.
- [7] Kraaijpoel D, Dost B (2013): Implications of salt-related propagation and mode conversion effects on the analysis of induced seismicity. *J. Seismol.*, **17**, 95-107, doi: 10.1007/s10950-012-9309-4.
- [8] Miraglia S, Courage W, Meijers P (2015): Fragility Functions for Pipeline in Liquefiable Sand: a Case Study on the Groningen Gas-Network. *12th International Conference on Applications of Statistics and Probability in Civil Engineering ICASP12*, Vancouver, Canada.
- [9] Cotton F, Archuleta R, Causse M (2013): What is sigma of stress drop? *Seismol. Res. Lett.*, **84** (1), 42-48, doi: 10.1785/0220120087.
- [10] Rodriguez-Marek A, Cotton F, Abrahamson N, Akkar S, Al-Atik L, Edwards B, Montalva G, Mousad H (2013): A model for single-station standard deviation using data from various tectonic regions. *Bull. Seismol. Soc. Am.*, **103**, 3149-3163, doi: 10.1785/0120130030.
- [11] Kotha SR, Bindi D, Cotton F (2016): Region, magnitude and site dependencies of response spectral values correlations and Conditional Mean Spectra, submitted.
- [12] Bazzurro P, Luco N (2005): Accounting for uncertainty and correlation in earthquake loss estimation. *ICOSSAR*, Millpress, Rotterdam, 2687-2694.
- [13] Akkar S, Bommer JJ (2010): Empirical equations for the prediction of PGA, PGV, and spectral accelerations in Europe, the Mediterranean Region, and the Middle East. *Seismological Research Letters*, **81** (2):195–206.
- [14] Anastasiadis A, Raptakis D, Pitilakis K (2001): Thessaloniki's detailed microzoning: subsurface structure as basis for site response analysis. *Pure and Applied Geophysics*, **158**, 2597-2633
- [15] Rathje E, Kottke A (2010): "Strata". <https://nees.org/resources/strata>.
- [16] Yang Z (2000): *Numerical Modeling of Earthquake Site Response Including Dilation and Liquefaction*. Ph.D. Dissertation, Dept. of Civil Engineering and Engineering Mechanics, Columbia University, New York, NY.
- [17] Chioccarelli E, Iervolino I (2013): Near-source seismic hazard and design scenarios. *Earthquake Engineering and Structural Dynamics*, **42**(4), 603-622, doi: 10.1002/eqe.2232.
- [18] Baltzopoulos G, Chioccarelli E, Iervolino I (2015): The displacement coefficient method in near-source conditions. *Engineering and Structural Dynamics*, **44**(7), 1015-1033, doi:10.1002/eqe.2497.
- [19] Akkar S, Cheng Y (2015): Application of Monte-Carlo simulation approach for the probabilistic assessment of seismic hazard for geographically distributed portfolio. *Earthquake Engineering and Structural Dynamics*, doi: 10.1002/eqe.2667.
- [20] Field EH, Biasi GP, Bird P, Dawson TE, Felzer KR, Jackson DD, Johnson KM, Jordan TH, Madden C, Michael AJ, Milner KR, Page MT, Parsons T, Powers PM, Shaw BE, Thatcher WR, Weldon II RJ, Zeng Y (2013): Uniform California Earthquake Rupture Forecast, version 3 (UCERF3) – The time-independent model. *U.S. Geol. Surv. Open-File Rept. 2013-1165*, California Geological Survey Special Report 228 and Southern California Earthquake Center Publication 1792.
- [21] Mignan A, Danciu L, Giardini D (2015): Reassessment of the Maximum Fault Rupture Length of Strike-Slip Earthquakes and Inference on M_{max} in the Anatolian Peninsula, Turkey. *Seismol. Res. Lett.*, **86** (3), 890-900, doi: 10.1785/0220140252.

- [22] Giardini D, Woessner J, Danciu L, Valensise G, Grunthal G, Cotton F, Akkar S, Basili R, Stucchi M, Rovida A, Stromeyer D, Arvidsson R, Meletti F, Musson R, Sesetyan K, Demircioglu MB, Crowley H, Pinho R, Ptilakis K, Douglas J, Fonseca J, Erdik M, Campos-Costa A, Glavatovic B, Makropoulos K, Lindholm C, Cameelbeec T (2013): Seismic Hazard Harmonization in Europe (SHARE): Online Data Resource. *Swiss Seismological Service Report*, Zurich, Switzerland, doi: 10.12686/SED-00000001-SHARE.
- [23] Uckan E, Akbas B, Shen J, Rou W, Paolacci F, O'Rourke M (2015): A simplified analysis model for determining the seismic response of buried steel pipes at strike-slip fault crossings. *Soil Dynamics and Earthquake Engineering*, **75**, 55-65, doi: 10.1016/j.soildyn.2015.03.001.
- [24] Mignan A, Wiemer S, Giardini D (2014): The quantification of low-probability–high-consequences events: part I. A generic multi-risk approach. *Nat. Hazards*, **73**, 1999-2022, doi: 10.1007/s11069-014-1178-4.
- [25] Mignan A, Danciu L, Giardini D (2016): Considering large earthquake clustering in seismic risk analysis. *Nat. Hazards*, in press, doi: 10.1007/s11069-016-2549-9.
- [26] Matos JP, Mignan A, Schleiss AJ (2015): Vulnerability of large dams considering hazard interactions: Conceptual application of the Generic Multi-Risk framework. *13th ICOLD Benchmark Workshop on the Numerical Analysis of Dams*, Lausanne, Switzerland, 285-292.
- [27] Babic A, Dolsek M (2014): The impact of structural components on fragility curves of single-storey industrial precast structures. *2nd European Conference on Earthquake Engineering and Seismology*, Istanbul, Turkey.
- [28] Casotto C, Silva V, Crowley H, Nascimbene R, Pinho R (2015): Seismic fragility of Italian RC precast industrial structures. *Engineering Structures*, **94**, 122-136, doi: 10.1016/j.engstruct.2015.02.034.
- [29] Iervolino I, Giorgio M, Chioccarelli E (2014): Closed-form aftershock reliability of damage-cumulating elastic-perfectly-plastic systems. *Earthquake Engineering and Structural Dynamics*, **43** (4), 613–625, doi:10.1002/eqe.2363.
- [30] Iervolino I, Giorgio M, Chioccarelli E (2016): Markovian modeling of seismic damage accumulation. *Earthquake Engineering and Structural Dynamics*, **45** (3), 441–461, doi: 0.1002/eqe.2668.
- [31] Kakderi K et al. (2015) Deliverable 4.2: Guidelines for performance and consequences assessment of geographically distributed, non-nuclear critical infrastructures exposed to multiple natural hazards. *STREST project EC/FP7* (2007-2013), grant agreement No: 603389.
- [32] Ptilakis K, Franchin P, Khazai B, Wenzel H, Eds (2014): SYNER-G: Systemic seismic vulnerability and risk assessment of complex urban, utility, lifeline systems and critical facilities. *Methodology and applications. Series: Geotechnical, Geological and Earthquake Engineering*, **31**, Springer, Netherlands.
- [33] Franchin P, Cavalieri F (2013): Seismic vulnerability analysis of a complex interconnected civil infrastructure, in S. Tesfamariam and K. Goda (eds.). *Handbook of Seismic Risk Analysis and Management of Civil Infrastructure Systems*, Woodhead Publishing Limited, Cambridge, UK.
- [34] Mignan A, Scolobig A, Sauron A (2016): Using reasoned imagination to learn about cascading hazards: a pilot study. *Disaster Prevention and Management*, **25** (3), 329-344, doi: 10.1108/DPM-06-2015-0137.
- [35] Lanzano G, Santucci de Magistris F, Fabbrocino G, Salzano E (2015): Seismic damage to pipelines in the framework of Na-tech risk assessment. *Journal of Loss Prevention in the Process Industries*, **33**, 159-172, doi: 10.1016/j.jlp.2014.12.006.
- [36] Esposito S, Stojadinović B, Babič A, Dolšek M (2017): Engineering risk-based methodology and grading system for stress testing of critical non-nuclear infrastructures (STREST Project). *16th World Conference on Earthquake Engineering*, January 9th to 13th 2017, Chile.